The Effects of Volcanic Aerosols on Mid-Latitude Ozone Recovery

Jessica D. Haskins

Submitted to the Department of Earth, Atmospheric and Planetary Sciences in Partial Fulfillment of the Requirements for the Degree of Bachelor of Science in Earth, Atmospheric, and Planetary Sciences at the Massachusetts Institute of Technology

May 19th, 2014
[June 2014]

Signature redacted

Author: _____

Department of Earth, Atmospheric, and Planetary Sciences
May 19, 2014

Signature redacted

Certified By: _____

Susan Solomon
Thesis Supervisor

Signature redacted

Accepted By: _____

Richard P. Binzel
Chair, Committee on Undergraduate Program

Abstract

In this paper, comparisons between the derived Chemistry Climate Model Initiative aerosol data set to balloon sonde measurements of aerosols made in Laramie, Wyoming are made between 1979-2012. Using the derived CCMI aerosol data set as the input for surface area density of aerosols in the Specified Dynamics-Whole Atmosphere Climate Community Model (SD-WACCM), the impacts of volcanic aerosols on mid-latitude ozone loss are investigated. These results are compared to the ozone column expected recovery from a run of SD-WACCM with no volcanic eruptions in the same period. Particular emphasis is placed on the last decade to investigate how the small volcanic eruptions that have characterized the period of 2008-2012 have impacted the ozone column recovery during this time at northern mid-latitudes as atmospheric chlorine levels decrease from regulation. It is found that the CCMI aerosol data set underestimates aerosol surface area density between the local tropopause and approximately 70mbar in the lower stratosphere. This underestimation is corrected and the resulting change in the ozone column is compared to the initial model output with no volcanic aerosols. Using the correct aerosol values, it is shown that ozone loss in the lower stratosphere after these small, recent volcanoes rivals that of the post-Pinatubo years around 1995-1996.

Acknowledgements

I would like to thank Susan Solomon for her guidance, support, and insight developing this project as well as her support as a mentor throughout my time as an undergraduate. I would also like to thank the rest of the Solomon group: Diane Ivey for her help in teaching me to use our server, for downloading terabytes of data from NCAR for use in this project, and for her assistance in reading in all of the data; Justin Bandoro and Daniel Gilford for their writing feedback, inspiration, and support in formatting the results. I'd like to thank Ryan Neely and Doug Kinnison at UCAR for setting up and running SD-WACCM with the inputs analyzed in this project and providing useful feedback throughout my project. Additionally, I'd like to thank all of the others within the EAPS and MIT community who made this project possible, including Jane Conner for writing instruction, Kathryn Materna for useful feedback on data presentation, and Grace Teo for writing criticism and support. Finally, I'd like to thank my family and friends for their ceaseless motivation.

Contents

List of Figures

1 Motivation

Ozone absorbs solar energy at wavelengths shorter than approximately 320nm and protects the biosphere from harmful solar radiation. This absorption prevents radiation-induced DNA damage in humans and animals known to cause skin cancer as well as eye cornea and lens damage [Brasseur & Solomon, 2005]. Because of these important health effects, it is important to understand how the ozone layer varies with anthropogenic and natural changes.

Ozone loss is strongly associated with chlorine, bromine, and other halogen levels in the atmosphere [Molina & Rowland, 1974; Solomon et al., 1996] Since regulation was enacted, the emissions of chlorofluorocarbons (CFCs) and other anthropogenic sources of atmospheric halogens have declined [Montzka et al., 2011]. There is significant scientific and political interest in determining whether the ozone layer has begun to recover because of this regulation of atmospheric halogens. As the levels of atmospheric halogens continue to decrease, the recovery of the ozone column to 1980 levels is expected to occur by 2030 at northern mid-latitudes [Austin et al. 2010; Erying et al., 2010a]. However, this recovery has not yet been observed, and ozone column levels have remained steady for the past decade. Increased levels of atmospheric aerosols, defined as any solid or liquid particles suspended in the air, are known cause stratospheric ozone loss [Wenneberg, et al. 1994; Solomon et al. 1996; Robok et al. 2010]. These aerosols provide surfaces upon which heterogeneous reactions occur using chlorine to deplete ozone. When the stratosphere has high surface area density from increased aerosol content, (e.g after a volcanic eruption) and chlorine levels are high, ozone loss is seen. As long as chlorine remains in high concentrations in the stratosphere, volcanic eruptions will play an important role in ozone loss through the reactions that take place on their surfaces [Tie and Brasseur, 1995, Solomon et al., 1996].

The past several years, from 2008-2012, have seen the eruptions of several small volcanoes causing increased levels of atmospheric aerosols. No very large eruptions have occurred since that of Mt. Pinatubo in 1991. Instead, the last two decades have been characterized by several small eruptions leading to persistently high stratospheric aerosol content [Nagai et al., 2010; Vernier et al., 2011; Neely et al., 2013;] including the Nabro eruption in Eritrea in 2011 that resulted in the largest stratospheric aerosol cloud since 1991[Bourassa et al., 2012]. This paper seeks, primarily, to understand the potential of role of the recent smaller volcanic eruptions on the ozone column above northern mid-latitudes. We ask, is the amount of ozone loss resulting from recent volcanic eruptions masking the expected recovery of ozone resulting from decreasing levels of atmospheric halogen levels? Do these small volcanic eruptions explain the stagnation of stratospheric ozone recovery over mid-latitudes? In answering this question, we employ a global climate model to understand the changing chemical background of the stratosphere from the period 1979-2012 under two different aerosol regimes: one including volcanic aerosols, and one without volcanic aerosols. By comparing these two runs, we seek to understand the impact that aerosols have had on ozone recovery as atmospheric halogens decrease. The validity of our aerosol inputs to the model is

examined using ground-based measurements and suggestions are made to improve the inputs and presented analysis.

2 Ozone Chemistry & Aerosols

Ozone production and loss in the stratosphere is driven by the coupling of several different, well-known radical catalytic loss cycles [Fahey et al., 1993; Wenneberg et al., 1994; Tie and Brasseur et al., 1995; Portmann et al., 1996; Solomon et al., 1996; Jacob, 1999; Tabazadeh et al., 2002; Brassuer & Solomon, 2005; Seinfeld & Pandis, 2006]. In such a cycle, ozone reacts with different substances that go on to rapidly reform all of the reactants except for ozone. Coupled in series, these reactions have a cumulative effect of depleting only ozone. Atmospheric aerosols don't directly impact ozone levels, but instead shift the balance between reactants that propagate these cycles. Therefore, understanding the coupling between these catalytic loss cycles is necessary to understand how different aerosol levels in the atmosphere affect ozone loss and how future changes in aerosol levels and the chemistry of the atmosphere may change these cycles.

2.1 HO_x catalyzed ozone loss

The rapid cycling of OH and HO_2, together known as the HO_x family can result in the catalytic loss of ozone. The initiation of ozone loss from hydroxyl radicals in the stratosphere, OH and HO_2, can occur through any chemical mechanism that generates OH or HO_2. Shown below, is one such step involving the oxidation of water vapor:

$$H_2O + O(^1D) \rightarrow 2OH \tag{1}$$

Upon creation, atmospheric OH can react with many atmospheric species, including ozone. OH and HO_2 cycle back and forth quickly with the net result of destroying ozone:

$$OH + O_3 \rightarrow HO_2 + O_2 \tag{2}$$
$$HO_2 + O_3 \rightarrow OH + 2O_2 \tag{3}$$
$$\text{Net: } 2O_3 \rightarrow 3O_2$$

This catalytic destruction of ozone is terminated with the reaction of the two radicals, OH and HO_2:

$$HO_2 + OH \rightarrow H_2O + O_2 \tag{4}$$

This ozone loss cycle is only persistent during the day because of the availability of OH. However, ozone isn't regenerated at night, so loss during the day is significant even though the loss cycle is

diurnal. It is important to note that when OH or HO_2 levels in the atmosphere are high, ozone loss increases from the increased occurrence of reactions 2 - 3. As will be discussed later, although atmospheric aerosol levels don't affect HO_x concentrations directly, they can increase the production of OH which leads to some enhanced ozone loss from reactions 2 - 3. HO_x concentrations don't vary too much throughout the stratosphere, so these reactions are roughly of equal importance to ozone loss in the upper and lower stratosphere.

2.2 ClO_x catalyzed ozone loss

Chlorofluorocarbons (CFCs), used commercially in refrigerants, were steadily added to the atmosphere in increasing amounts after WWII where they could remain inert in the troposphere for 40-150 years. However, upon exposure to high-energy photons in the stratosphere, CFCs photolyze and produce significant amounts of chlorine that propagate another catalytic ozone loss cycle [Molina & Rowland, 1974]. For example, the photolysis of CFC-12 (commonly, used in vehicle air conditioners before regulation):

$$CF_2Cl_2 + h\nu \rightarrow CF_2Cl + Cl \tag{5}$$

Upon release, the chlorine atoms trigger a catalytic ozone loss cycle. Cycling between Cl and ClO occurs so rapidly that this ensemble is referred to as ClOx. The net effect of this rapid cycling is only the destruction of ozone since both ClO and Cl are regenerated:

$$Cl + O_3 \rightarrow ClO + O_2 \tag{6}$$

$$ClO + O \rightarrow Cl + O_2 \tag{7}$$

$$\text{Net: } O_3 + O \rightarrow 2O_2$$

The cycle is terminated through conversion of molecular chlorine to its reservoir species, HCl, HOCl, and $ClNO_3$. These species are longer-lived and more inert than molecular chlorine. Effectively, a molecule of chlorine that was formerly available to continually go around this cycle depleting ozone (hereafter 'reactive chlorine') is removed from the system by conversion to its reservoir species. Therefore, the conversion of reactive chlorine into these reservoir species represents a decline in the rate of ozone loss.

$$Cl + CH_4 \rightarrow HCl + CH_3 \tag{8}$$

$$ClO + HO_2 \rightarrow HOCl + O_2 \tag{9}$$

$$ClO + NO_2 + M \rightarrow ClNO_3 + M \tag{10}$$

Bromine is also an important atmospheric halogen and can lead to very similar catalytic loss of ozone through formation of BrO and Br molecules. It also has similar reservoir species, $BrONO_2$,

HOBr, and HBr. Because bromine is a larger molecule than chlorine, the energy needed to break its bonds is lower. As a result, bromine compounds cycle more quickly than chlorine causing bromine to have higher ozone depletion potential than chlorine. Luckily, bromine concentrations in the atmosphere are significantly lower than chlorine, but its contributions to ozone loss cannot be ignored. Although the bromine catalyzed ozone loss process isn't detailed here because of its similarities to chlorine, its contributions can not be ignored in a robust calculation of ozone loss from aerosol enhancements. One of the most important reactions in the lower stratosphere that couples the BrO_x and ClO_x ozone loss cycles is:

$$BrO + ClO \rightarrow Br + Cl + O_2 \tag{11}$$

Unlike the ClO_x reactions describe above (6-7), this process does not need O to propagate ozone loss. O comes from the photolysis of O_2 at wavelengths $\nu < 242$ nm:

$$O_2 + h\nu \rightarrow O + O \tag{12}$$

Because of the high energy photons needed to dissociate O_2, not much O exists in the lower stratosphere, but is in higher concentrations as one moves up through the atmosphere. Where these higher energy photons are more prevalent. The same is true of Cl, Br, ClOand BrO in the stratosphere. Although, the rate limiting step to reactions 6-7 is the amount of available O. Thus, reaction 11 contributes to ozone loss in the lower stratosphere more than reactions 6-7 and their BrO_x counterparts. The variation of O and ClO among other ozone relevant atmospheric constituents are shown in Figure 1.

2.3 NO_x catalyzed ozone loss

Ozone loss can also occur through a catalytic cycle involving NO and NO_2. Cycling between NO and NO_2 takes place on a time scale of about one minute during the daytime in the stratosphere (13 - 16). Because of the rapid exchange between the two species, the chemical family of NO and NO_2 is defined as NO_x. One important note is that because of reaction 14, any substantial loss process that depletes O will also deplete ozone. Therefore, we refer to the odd oxygen family, O_x as O and O_3 together. Together these 4 reactions make up the NO_x catalyzed ozone loss cycle:

$$NO_2 + h\nu \rightarrow NO + O \tag{13}$$

$$O + O_2 \rightarrow O_3 \tag{14}$$

$$2x \quad \left(NO + O_3 \rightarrow NO_2 + O_2\right) \tag{15}$$

$$NO_2 + O \rightarrow NO + O_2 \tag{16}$$

$$\text{Net: } 2O_3 \rightarrow 3O_2$$

The NO_x cycle only perpetuates during the day because the photolysis of NO_2 (13) stops at night, and all of the remaining NO quickly reacts with O_3 to form NO_2 at sunset (15). The cycle can be terminated during the day when NO_x is converted to its reservoir species, HNO_3. Thus, when levels of reservoir species are higher, there is less reactive nitrogen available to deplete ozone. During the day, NO_2 reacts with OH to form the daytime reservoir species, nitric acid, HNO_3:

$$NO_2 + OH \rightarrow HNO_3 \tag{17}$$

The mechanism only allows the loss of reactive nitrogen to its reservoir species, HNO_3 during the day. This is because OH is formed from the reaction of water with $O(^1D)$ (1) which only occurs during the daytime because of the availability of $O(^1D)$. After sunset, $O(^1D)$ is not formed, and, therefore, OH is not produced. However, loss of reactive nitrogen still occurs at night through the oxidation of NO_2 by O_3 (18) and subsequent conversion to its nighttime reservoir species, N_2O_5 (19):

$$NO_2 + O_3 \rightarrow NO_3 + O_2 \tag{18}$$

$$NO_3 + NO_2 \rightarrow N_2O_5 \tag{19}$$

NO_3 is very photolytic and is quickly converted back to its reactants during the day. Therefore, the conversion of reactive nitrogen to the N_2O_5 reservoir species is only important at night. The reservoir species, N_2O_5 and HNO_3, are non-radical species and have relatively long lifetimes against chemical loss, but are eventually converted back to NO_x through photolysis:

$$HNO_3 + h\nu \rightarrow NO_2 + OH \tag{20}$$

$$N_2O_5 + h\nu \rightarrow NO_2 + NO_3 \tag{21}$$

Both of these reservoir species only represent a temporary removal of NO_x from the system. However, HNO_3 removes NO_x from the system on the order of a few weeks and N_2O_5, a few hours [Jacob, 1999]. Together, NO_x and its reservoirs, HNO_3 and N_2O_5, are defined as the chemical family, NO_y. The NO_x/ NO_y ratio gives information on the amount of reactive nitrogen available to the total amount of nitrogen, including the reservoir species. When the NO_x/NO_y ratio is small, more nitrogen is tied up in its more inert, reservoir species and there is less reactive nitrogen available to propagate ozone loss through the NO_x catalytic cycle. When this ratio is larger, more reactive nitrogen is available, and more ozone loss is seen. This ratio does vary with altitude and controls ozone chemistry at different levels in the atmosphere. Figure 1 shows the variation of the constituents that make up NO_x in red and those that make up NO_y in blue. Since the NO_x catalytic cycle is driven by reactions with O, this cycle is less important in the lower stratosphere where there is less O, but is the primary mechanism for upper stratospheric ozone loss. Additionally,

the lifetime against photolysis of HNO_3 decreases with height because of the availability of higher energy photons. So, in the upper stratosphere, the NO_x/ NO_y ratio is generally higher than in the lower stratosphere. So ultimately, we expect the NO_x catalytic cycle to be the main driver of ozone loss in the upper stratosphere, and the ClO_x+BrO_x coupled catalytic cycle to be that in the lower stratosphere.

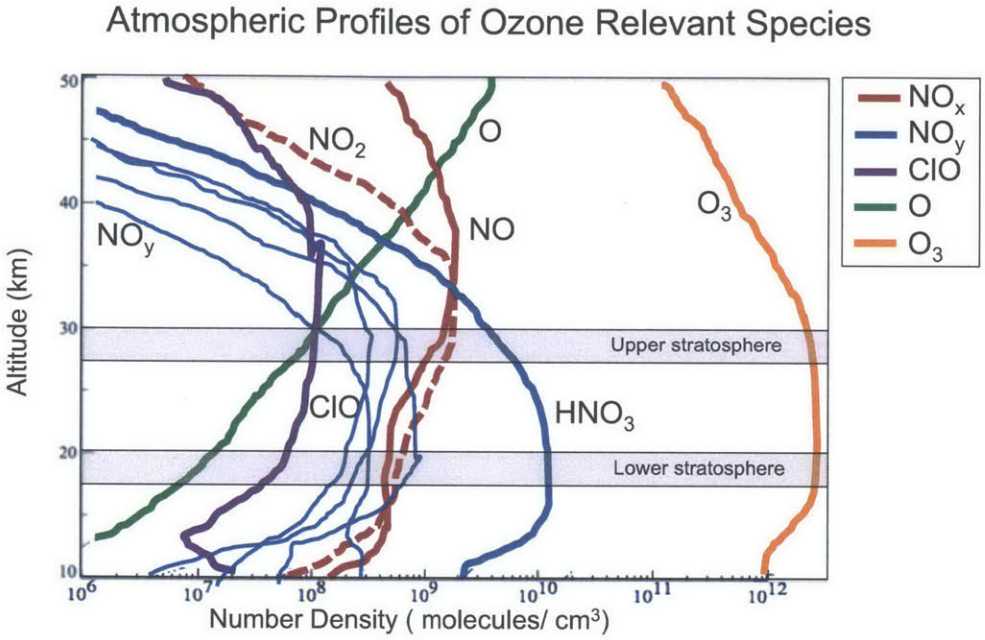

Figure 1: Shown above is the number concentration of different atmospheric species as a function of altitude. In the box around the lower stratosphere, the NO_x/ NO_y ratio is smaller than in the box around the upper stratosphere because of the concentration of O. In the lower stratosphere, the loss cycle from ClO+ BrO which doesn't need O to propagate is more important. In the upper stratosphere, the NO_x loss cycle is more important because of the increased photolysis of HNO_3 and availability of O. From JPL, 1997.

2.4 Heterogeneous Chemistry on Aerosols

In volcanic years, the concentration of aerosols in the atmosphere increases because of aerosols being thrust there by volcanic emissions. Water vapor condenses on these aerosols and allows for heterogeneous reactions between gaseous species and liquid water to take place. Although the water vapor content of the atmosphere may not increase in volcanic years, so less water is on each particle, it is the increased surface area that matters because there is more total area that the water on the particles can interact with the gaseous species in the air. A common measure of the amount of aerosols sites available for reactions is called surface area density (SAD) and is typically measured in $\mu m^2 cm^{-3}$- or the surface area available for these reactions to take place in a volume of air. In volcanic years when SAD is higher, there is an increased amount of $H_2O(\ell)$ available for reaction

because of water vapor condensing on the extra aerosols. The major heterogeneous reaction linking aerosol changes to ozone depletion at mid-latitudes is the hydrolysis of N_2O_5:

$$N_2O_5 + H_2O(\ell) \rightarrow 2HNO_3 \tag{22}$$

This reaction proceeds more rapidly in volcanic years when more $H_2O(\ell)$ is available. From the standpoint of the NO_x catalyzed ozone loss mechanism discussed above, this reaction simply converts nitrogen from the nighttime reservoir species to the daytime reservoir species. However, HNO_3 is a longer-lived NO_xreservoir species than N_2O_5, so that conversion slows down the regeneration of NO_x.This means that in volcanic years where SAD is high, the amount of available NO_x for reaction goes down. Based solely on the NO_x catalyzed ozone loss cycle discussed above, one would expect ozone loss to be suppressed since there would be less total reactive nitrogen to destroy ozone (13 - 16). In the upper stratosphere, where the NO_x catalyzed loss cycle is the most important, the lowering of NO_x/ NO_y ratio ratios leads to the creation of ozone. However, in the lower stratosphere, the coupling with the ClO_x, BrO_x and HO_x catalytic loss cycles makes the effect on ozone in the lower stratosphere more complicated. The two different effects in the upper and lower stratosphere must be added together to get the net effect on the ozone column which is the total amount that affects how much radiation makes it to the surface impacting human health.

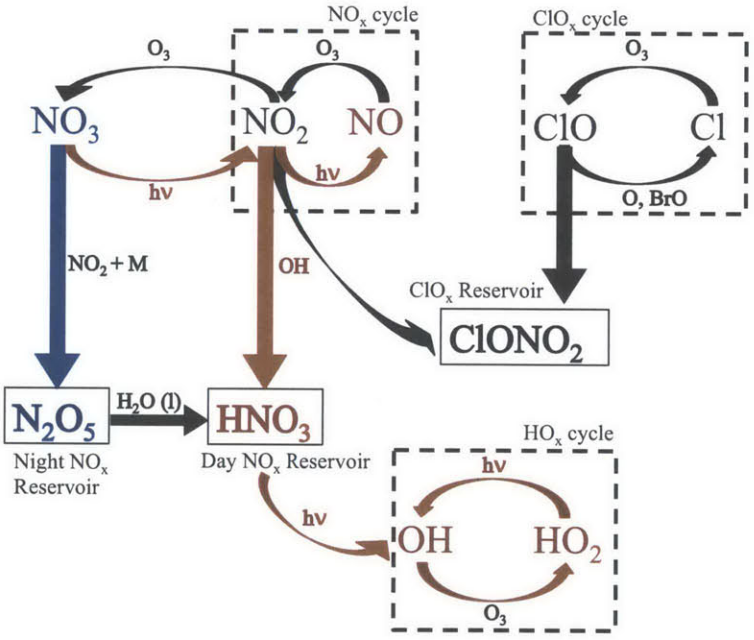

Figure 2: A visual representation of the coupling of the HO_x, ClO_x, NO_x catalytic ozone loss cycles. Light sensitive reactions and molecules are shown in orange. Processes that dominate at night are shown in blue.

One of the terminating steps in the ClO_x cycle, is the reaction of ClO with NO_2 (10). With

less total available NO_x, this reaction will slow. So, the amount of chlorine in its reservoir species, $ClONO_2$ will decrease meaning that the amount of reactive chlorine available to deplete ozone will increase. Thus, we expect to see an increase in the amount of ozone depletion from the ClO_x catalyzed ozone loss cycle and a decrease in the amount of ozone depletion from the NO_x catalyzed ozone loss cycle. However, this reaction shifting N_2O_5 to HNO_3 also has other ramifications on the HO_x catalyzed ozone loss cycle. Both NO_x reservoir species are eventually photolyzed and return NO_x to the system (20 & 21). The important distinction is that the photolysis of N_2O_5 only returns NO_x while the photolysis of HNO_3 returns both NO_x and OH. So, reaction 22 also has the effect of increasing OH levels. With more available, OH, we expect to enhance the HO_x catalyzed ozone loss cycle leading to more ozone loss.

To summarize, aerosols affect the partition of stratospheric nitrogen by the enabling the nighttime NO_x reservoir, N_2O_5 to be converted to the daytime NO_x reservoir. This reaction lowers NO_x levels which decreases ozone loss from the NO_xcycle thereby increasing the total amount of ozone in the upper stratosphere. Lower NO_xlevels inhibit the ability of ClO_x to be converted to its reservoir species, such that ClO is longer lived in the atmosphere. Therefore, ozone loss from the ClO_x catalyzed cycle increases, and the total amount of ozone decreases in the lower stratosphere. Reaction 22 also enables extra release of OH which increases ozone loss from the HO_x catalyzed cycle thereby decreasing the total amount of ozone. Figure 3 shows the steps through which ozone is affected resulting from reaction 22.

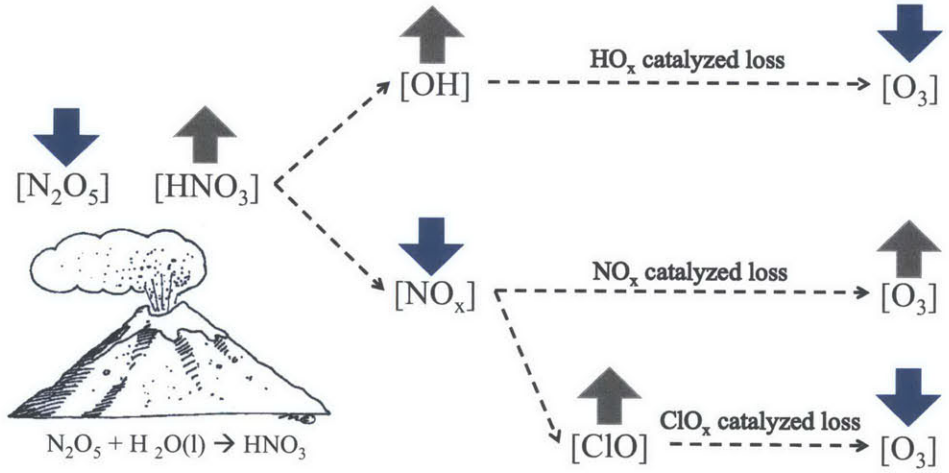

Figure 3: A visual summary of the expected, qualitative effects on ozone that the conversion of N_2O_5 to HNO_3 causes.

While the contribution from each of the cycles on ozone levels is understood qualitatively, in order to understand the net effect on ozone levels, a quantitative understanding is needed. For example, if the ozone increase resulting from the NO_x cycle in the upper stratosphere is larger than the sum of the ozone decreases from the ClO_x and HO_x cycles in the lower stratosphere then, we

would expect to see a total increase in column ozone. A previous study was done using a simple model with the above chemistry to understand which of the effects on ozone was most significant in the mid stratosphere. It was found that in the mid stratosphere, the enhancements made to the ClO_x cycle made the largest contributions to the loss of ozone, HO_x enhancements were nearly negligible, and contributions from the NO_x cycle were significant, but less so than that of ClO_x [Solomon et al., 1996]. Figure 4 from Solomon et al., 1996 shows how the ClO_x cycle dominates the net effect on ozone from SAD enhancements.

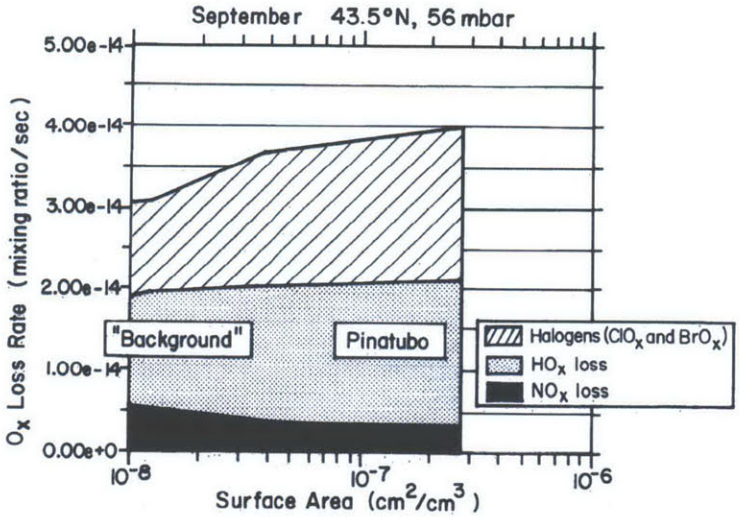

Figure 4: Comparison of the contributions from the ClO_x, HO_x and NO_x cycles to the odd oxygen loss rate as a function of surface area for 1990 levels of total chlorine and bromine. From Solomon et al., 1996.

These results indicate that because halogen related catalytic cycles are responsible for the majority of ozone depletion at this level, that even a small shift in levels of atmospheric halogens can have substantial impacts on ozone loss. In the period just after the El Chichón volcanic eruption, it was shown that increasing stratospheric chlorine and bromine levels approximately canceled the effect of decreasing aerosol content, giving rise to the relatively constant ozone losses observed from about 1986-1989 [Solomon et al., 1996]. The above comparisons between contributors to the O_x loss rate were made using the chlorine and bromine levels of 1990. Regulation has since caused the emissions of CFCs and other anthropogenic halogens to decline slightly [Montzka et al., 2011]. Both the public and scientific community have been waiting for the recovery of the ozone column as ClO_x catalyzed ozone loss decreases in the lower stratosphere. However, this expected recovery of column ozone has not been observed. In order to examine the possible effect that recent small volcanic eruptions may have played on the ozone column, we must reconsider the quantitative balance between the catalytic loss cycles with the appropriate levels of atmospheric chlorine and bromine. We must also separate and consider the different regimes leading to ozone

loss in the lower stratosphere and ozone creation in the upper stratosphere after these volcanic eruptions quantitatively to understand the total effect on the ozone column.

3 Model & Methods

In order to consider the quantitative balance between all of the catalytic cycles linking atmospheric aerosol levels to ozone loss throughout the stratosphere, a global chemistry climate model, the Specified Dynamics-Whole Atmosphere Community Climate Model (SD-WACCM) is used. Input for aerosols into the model are taken from the Chemistry Climate Model Initiative (CCMI) Aerosol Data Set. Balloon measurements of aerosols taken in Laramie, Wyoming are used to verify the CCMI aerosol data set as an input into SD-WACCM. Information on each of these data sets and the model used to simulate atmospheric chemistry is given below.

3.1 Specified Dynamics-Whole Atmosphere Community Climate Model

The Specified Dynamics-Whole Atmosphere Community Climate Model (SD-WACCM) was used to probe the effects on stratospheric ozone from different aerosols. SD-WACCM is a comprehensive numerical model spanning the range of altitude from the Earth's surface to the thermosphere updated and operated out of the National Center for Atmospheric Research (NCAR). Its specified dynamics reproduces winds and temperatures from reanalysis data as to allow variation only in the chemistry between the two runs. Further information on the model can be found at: `http://www2.cesm.ucar.edu/working-groups/wawg`. In order to understand chemical differences in the atmosphere arising from different aerosol concentrations, we did two separate runs of SD-WACCM with different aerosol loadings over the period from 1979-2012; one with observed aerosol concentrations (including volcanoes) and one with only background aerosols (without volcanoes). The two different aerosol profiles used in our two SD-WACCM runs can be seen in Figure 5 over mid-latitudes at 85mbar. Only varying the aerosols fed into SD-WACCM will allow us to consider the chemical changes occurring in the atmosphere from aerosols alone since chlorine levels have also varied with time.

3.2 Chemistry Climate Model Initiative Aerosol Data Set

Having a valid representation of aerosols to feed into our model is important to simulate realistic chemical changes in the atmosphere. However, a continuous observational record of aerosol concentrations and surface area densities from volcanoes and other sources is hard to define because of satellite failures, differences in instrumentation and calibration, and inherent gaps. Unsurprisingly, the red line shown in Figure 5 is not strictly from one observational data set, but is from a derived data set with measurements from several different satellites and ground based instruments. There have been several attempts to create a continuous, global stratospheric aerosol

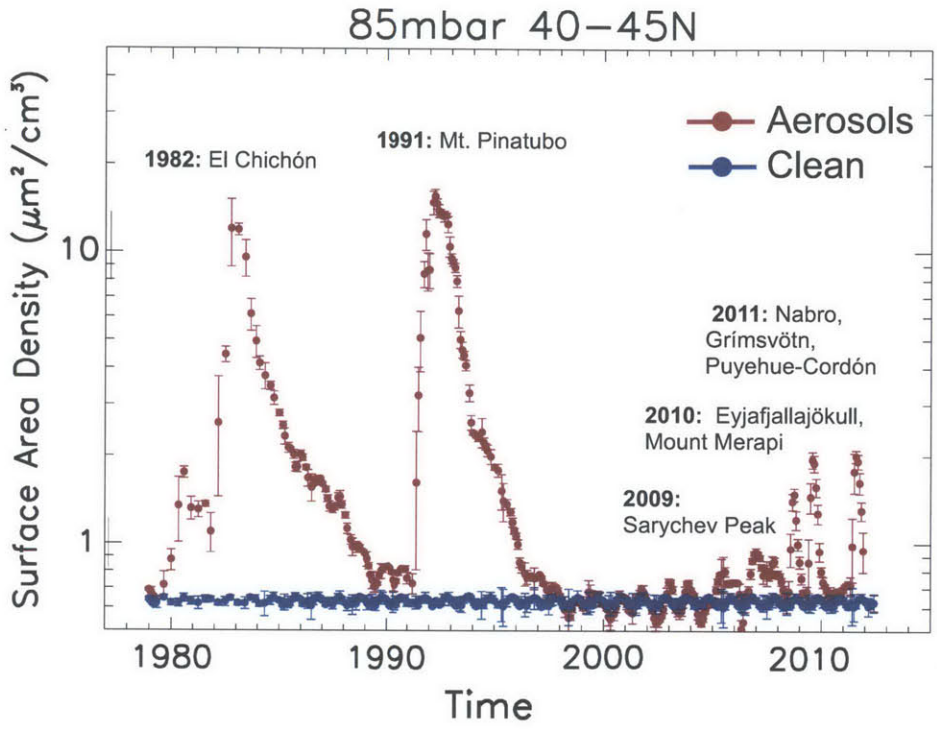

Figure 5: The time series shown in red is the aerosol data from observations and includes all volcanic eruptions that occurred in the period 1979-2010. The aerosol time series shown in blue is the 'clean' aerosol data set, which contains only background levels of SAD under the assumption that no volcanic eruptions happened in this period. These results are taken from the mid-stratosphere.

data set for use in climate models (e.g., Sato et al., 1993; Stenchikov et al., 1998). The most recent attempt to do so by Arfeuille et al. 2013 has been implemented and updated by the Chemistry Climate Model Initiative (CCMI). We use the CCMI aerosol data set with observed aerosols to force SD-WACCM which is shown in red in Figure 5. This data can be found at: `ftp://iacftp.ethz.ch/pub_read/luo/ccmi/`. In the time period 1979-2012, CCMI aerosol data set uses observed aerosol extinction coefficients from various satellites to derive the aerosol SAD. An empirical relationship between the observed extinction coefficients observed from the SAGE II satellite and aerosols surface area density was derived by Thompson et al. 1997. The core assumption behind the empirical relationship connecting observed extinction coefficients to surface area density is that the wavelength dependence of the extinction is stable for different aerosol extinctions. It is noted in Arfeuille et al. 2013 that this assumption was violated after the Mt. Pinatubo eruption in the lower tropical stratosphere because of both the small aerosol size and large extinction after the eruption. In a case where volcanic eruptions cause large changes in the size distribution of aerosols, the assumption can be violated and such a back calculation of SAD from extinction coefficients

may differ from the actual SAD. It is also important to note that the CCMI aerosol data are reliable only above the local tropopause. The CCMI aerosol data set uses observed aerosol extinction coefficients at 1020nm from the SAGE I satellite in the period 1979-1980 to derive the aerosol SAD using the method described above. It does the same with extinction coefficients at 1020nm from the SAM II satellite between 1981-1984 and with extinction coefficients at 1020nm, 525nm, 452nm, and 386nm from the SAGE II satellite between 1984-2005. Between the end of SAGE II measurements and the beginning of the CALIPSO satellite measurements from September 2005- June 2006, the annual mean of 2005 SAGE II data is used to forward extrapolate until April 2006, and is joined with the backward extrapolation from the first CALIPSO data point (June 2006) back into May 2006. After 2006, the extinction coefficients at 532nm from CALIPSO are used. However, the lidar ratio used to convert the CALISPO backscatter coefficients into extinction coefficients was derived from a look up table of zonal mean lidar ratios constructed with collocated measurements from the satellite GOMOS and CALISPO during the period from 2006-2009. The entire CCMI aerosol data set, once all of these satellite observations are compiled is shown in Figure 6 over mid-latitudes.

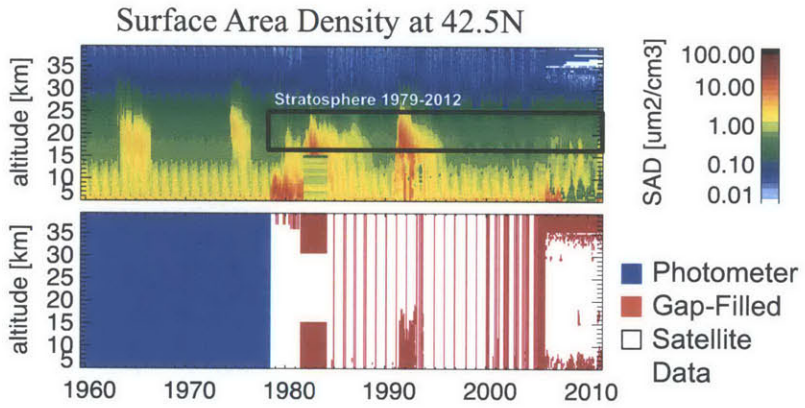

Figure 6: The CCMI aerosol data set as a function of time of derived aerosol surface area density used to force SD-WACCM is shown in the top panel. The source of the data and gap filling information is seen in the bottom panel. A cross section of this at a specific pressure level is shown after its input in SD-WACCM in Figure 5 .

3.3 Laramie, Wyoming Balloon Sondes

In situ balloon-borne measurements at Laramie, Wyoming (41^oN) have been taken from 1971-2014, making it the longest continuous record of tropospheric and stratospheric aerosols available. The measurements use two optical particle counters to measure aerosols $\geq$ 0.15, 0.25 μm and aerosols $\geq$ 0.15-2.0 μm in twelve size classes. Although there have been a few instrument changes over the record, all instrument changes provide continuity of the fundamental measurements of aerosols $\geq$ 0.15, 0.25 μm. These measurements are used to establish size distributions of

the aerosols as a function of altitude after which the surface area density, volume and extinction can be easily calculated [Deshler et al., 2002]. These measurements are taken from the surface to approximately 10mbar. Temperature, pressure, NO_2, and SO_2 measurements are also made. Data is available at `ftp://cat.uwyo.edu/pub/permanent/balloon/Aerosol_InSitu_Meas/US_Laramie_41N_105W/SizeDist_Stratosphere/`

Unlike the measurements for the CCMI calculations where size distributions are assumed after extinction coefficients measured to back calculate surface area, these measurements represent a more robust calculation since the size distribution is directly measure. Volcanic eruptions altering the size distribution assumption and thus, changing the calculated surface area density is not a problem for these in situ balloon measurements. Unlike satellite measurements, however, this data set cannot provide the same sort of spatial coverage, but can be compared to the CCMI data set around 41°N. However, offsets between the satellite data comprising the CCMI data set and the Laramie, Wyoming data set during volcanic periods is likely to be a good proxy for all latitudes. This assumption makes the comparison between these two data sets an important verification for the values of SAD from the CCMI aerosol data set.

Deshler et al. 2002 compared inferred aerosol surface areas from these in situ measurements and from SAGE II between 1984-2000. It was found that the agreement between these two independent measurements was within measurement uncertainty for aerosol surface area of volcanic aerosol, but for background aerosol the SAGE II surface areas were about 40% low. After comparing the differential surface area and extinction distributions it was found that in background conditions, aerosol sizes, which control surface area distributions, were below those which control extinction. They concluded that visible extinction measurements in non-volcanic periods could provide a poor representation for surface area, with a tendency to underestimate it [Deshler et al., 2002].

Understanding the limitations of satellite instruments to adequately measure aerosol surface area density, we use the Wyoming balloon measurements to verify the CCMI aerosol data set as input to SD-WACCM. Shown in Figure 7 is a comparison of the surface area density between SAGE II, CCMI, and Wyoming balloon measurements. We extend the comparisions made by Deshler et al. 2002 to the later volcanic period through 2012. The average cold point tropopause over the averaging period from the Wyoming balloon data is marked in black showing the boundary below which CCMI data shouldn't be used. The selected years are those after the El Chichón eruption (1982-1985), the Mt. Pinatubo eruption (1992-1995), the non-volcanic period (2000-2003) and the recent volcanically active period (2009-2011). We can see immediately that the retrieval algorithm for the CCMI aerosol data set takes care to account for the underestimations of SAGE II during non-volcanic years in its calculations since it agrees much more with the Wyoming SAD measurements between 2000-2003. However, we notice that in nearly all of the volcanic periods (except 1994-1995), between the local tropopause and about the 100mbar level, in the lower stratosphere, there is some disparity between the Wyoming and CCMI surface area densities. Consistently, the CCMI

data underestimates the surface area density in the lower stratosphere between the local tropopause and approximately 85mbar. Here, it is important to note that the surface area densities inputted into the model may be lower than actual surface area densities.

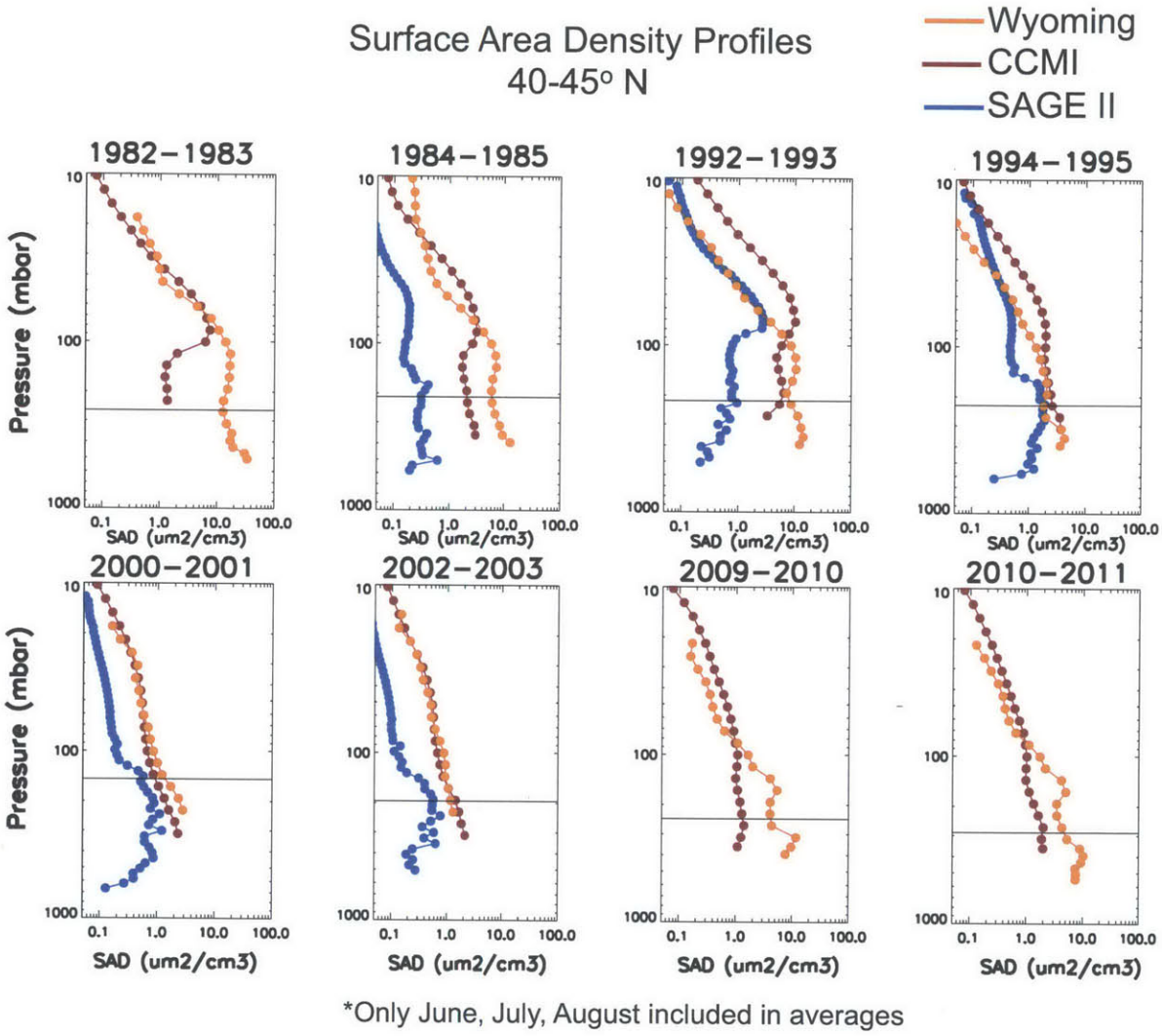

Figure 7: Two year averages are shown with only data taken in June, July, or August included in the averages. SAGE II and CCMI data is taken only between 40-45°N and Wyoming at 41°N. SAGE II data ends in 2005 and is not shown in subsequent years. The cold point tropopause average level is shown in black from Wyoming balloon measurements.

Although we initially intended this comparison merely to verify our model input, this comparison in itself is an important result since the CCMI aerosol data set is widely used in climate models. From these comparisons, we believe the CCMI aerosol data set that we used to force SD-

WCCM underestimates the true surface area density in the lower stratosphere by about a factor of 1.5-3, which is unexplained by previous works in the literature in the late period after 2005 when CALIPSO data is used to measure extinction coefficients and back out SAD measurements in the CCMI aerosol data set. A scaling factor that will be used later was derived at each pressure level for each year to describe the amount by which the CCMI aerosol data set underestimates the Wyoming SADs. This scaling factor can be seen in full in subsection 7.1 Underestimated SADs in this data set can have important radiative effects in the lower stratosphere as well as chemical effects. The significance of the differences between the CCMI aerosol data set used to force SD-WACCM and the Wyoming balloon sondes in relation to our chemical study will be discussed further below.

4 Results

4.1 Column Ozone Effects from Volcanic Aerosols

The percent change in column ozone values from January 1979 of the two separate SD-WACCM runs are shown below Figure 8. A 25-month running average was used to ignore effects from the quasi-biannual oscillation (QBO), which is a dynamic effect that mixes stratospheric ozone and occurs in a 2-year cycle. The top panel shows column ozone values if no volcanoes had gone off during the period 1979-2012 in blue and the column ozone values with volcanic eruptions in red using SADs from the CCMI aerosol data set. The bottom panel shows the difference in percent change of column ozone between the two lines. Numerically, the values in the bottom panel are taken from subtracting the values of the ozone column with volcanoes (red line) from the ozone column without volcanoes (blue line). When the percent change in ozone column between the two cases in the bottom panel is positive, the SD-WACCM run with aerosols showed less total ozone than the run without aerosols did.

In the volcanic periods of El Chichón (1982-1985) and Mt. Pinatubo (1992-1995), the difference in column ozone is apparent. The SD-WACCM run including the aerosols shows significantly more total ozone depletion than the run excluding those aerosols. Although the El Chichón and Mt. Pinatubo eruptions ejected roughly similar amounts of aerosols into the stratosphere over northern mid-latitudes, more ozone depletion is seen following the Mt. Pinatubo eruption due to the increased chlorine levels during that period. In the later volcanic period from 2008-2012, the top panel shows very little difference between the two runs. The anomaly plot shows about a 0.25% decrease in the ozone column between two runs. This is only a slight decrease in the total column when compared to the quiescent period with nearly no volcanic eruptions between 2000-2008 where the ozone column results roughly agree. These results alone indicate that the small volcanic eruptions did have an effect on decreasing the total ozone column, but the significance of this effect is debatable. However, knowing that CCMI aerosol data set is an underestimation of aerosol surface area density in the lower stratosphere where much of the ozone loss chemistry takes

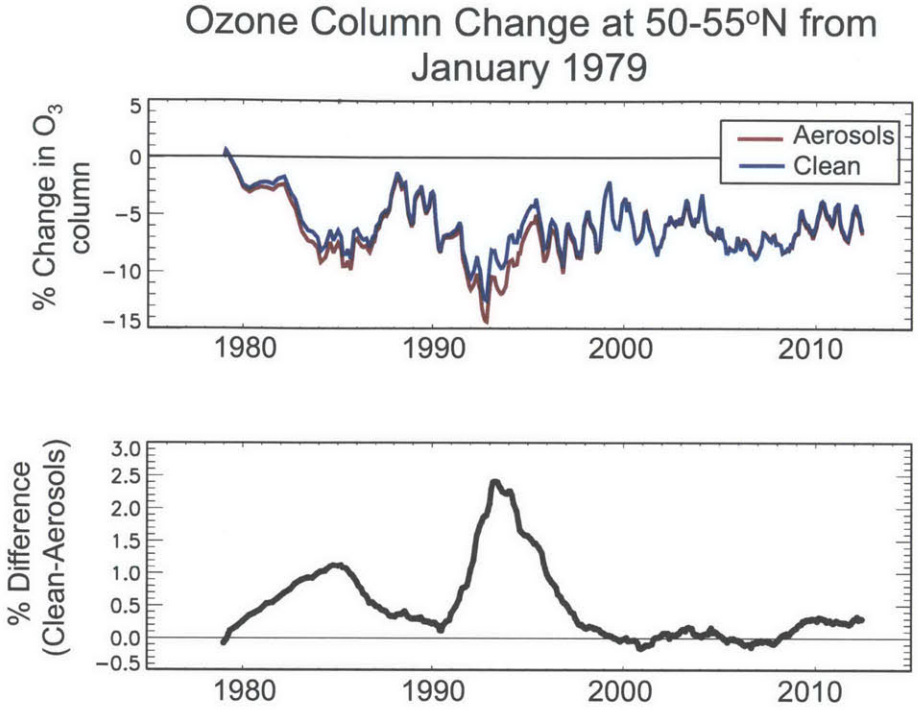

Figure 8: SD-WACCM predictions of column ozone over 50-55^o N for the two cases with aerosols (red) and without (blue) are shown in the top panel. The bottom panel shows the anomaly between the two cases.

place it must be understood that this flaw would cause the model to underestimate the effects on ozone depletion.

The total column ozone results ignore the different processes leading to ozone creation and ozone production in the lower and upper stratosphere, respectively. Perturbations could cause ozone loss in the lower stratosphere and production in the upper stratosphere that canceled one another in column measurement indicating that, chemically, such a perturbation is impactful. Figure 9 shows the percent difference in ozone as a function of pressure between the clean and aerosol run. In shades of orange are the El Chichón years, in blue are the Mt. Pinatubo years, and in green are the recent, volcanic years. The ozone column time series in Figure 8 is a sum of the losses of ozone in the lower stratosphere and ozone production in the upper stratosphere shown in Figure 9.

The differences seen in the profile of ozone is indicative of the varying NO_x levels in the upper and lower stratosphere discussed in previous sections. As expected, heterogeneous chemistry on the surface of volcanic aerosols lowers the NO_x levels throughout the stratosphere. In the lower stratosphere, where reaction 11 is the dominant ozone sink, this change leads to longer lifetimes of ClO and BrO, thereby increasing ozone loss through in the lower stratosphere. However in the upper stratosphere where the NO_x catalytic cycle is dominant, the lowering of NO_x levels

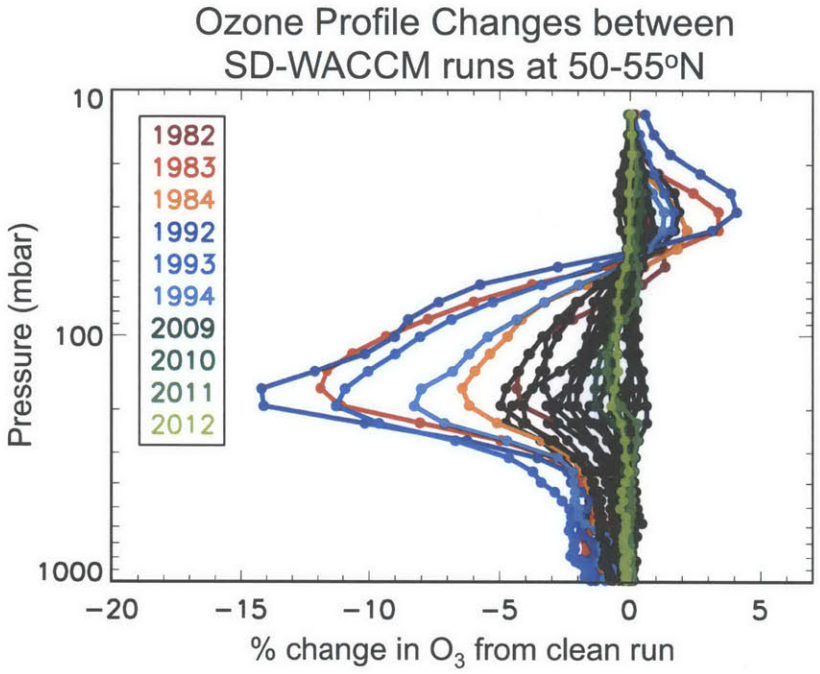

Figure 9: Percent difference between the SD-WACCM predictions of ozone at different pressure levels over 50-55^o are shown. Ozone loss is shown in the lower stratosphere and production in the upper stratosphere resulting from different NO_x/ NO_y ratios.

from heterogeneous chemistry on aerosols leads to decreased efficiency of the cycle, and thus, ozone production in this region during volcanic years. Figure 9 indicates that the El Chichón and Pinatubo eruptions saw large decreases in lower stratospheric ozone and increases in upper stratosphere ozone, but the more recent volcanic years saw neither large lower stratospheric reductions nor large increases in upper stratospheric ozone comparable to those years enhancements.

Figure 10 shows surface area density, ozone, and chlorine in the upper stratosphere at 21mbar and the lower stratosphere at 100mbar between the two SD-WACCM runs. A 25-month running average was used. It can be seen that ozone enhancements between the two runs at the 21mbar level during the recent volcanic period in 2008-2012 are more pronounced than the ozone losses at the 100mbar level. Although integrated through the column, these changes nearly cancel one another from the results shown in Figure 8.

Together, Figure 8 and Figure 9 indicate that SD-WACCM does not predict large chemical changes in the ozone column from the small aerosol perturbations in the recent volcanic period from either the dominant $ClO_x$and BrO_xreactions in the lower stratosphere nor the NO_x cycle in the upper stratosphere. However, since the CCMI data set underestimates the surface area density of the aerosols during this period specifically, the total depletion of ozone could be larger that what is predicted in the model. To understand how much of an effect underestimating these surface area

densities would have on the total ozone column the changes in different ozone relevant constituents is investigated as a function of surface area density.

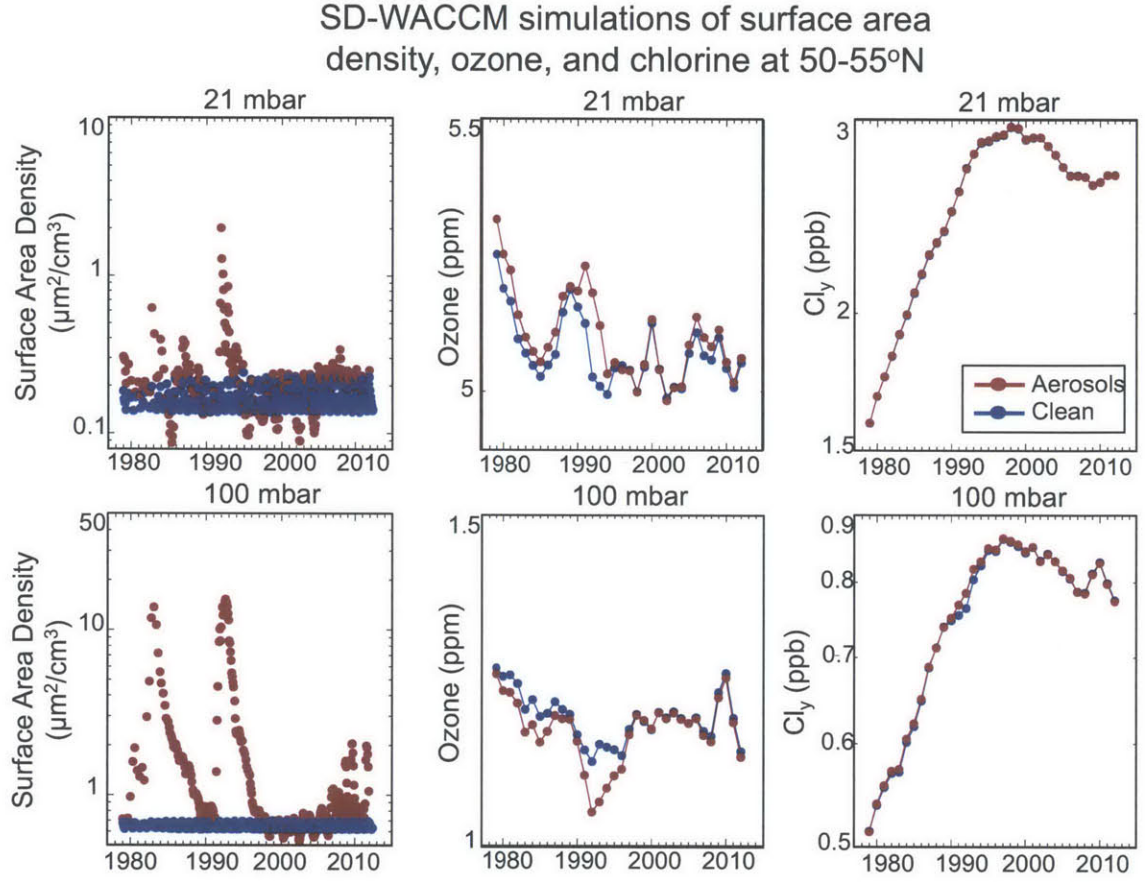

Figure 10: Ozone enhancements at 21mbar in the late volcanic period between the two runs are comparable to those after the El Chichón eruption. Little difference in ozone loss is seen during the recent volcanic period in the lower stratosphere.

4.2 Nonlinear Chemical Responses to Increased SAD

In Figure 11, three different ratios are shown at 21mbar in the upper stratosphere and 100mbar in the lower stratosphere. The values shown are obtained by taking the average ratio within a specified bin of surface area density from every individual ratio measurement made in June, July, and August between 1979-2012 with a solar zenith angle <45. The bin edges are defined as follows in $\mu m^2\ cm^{-3}$: [0.1, 0.4, 0.5, 0.6, 0.7, 0.8, 0.9, 1.0, 1.5, 2, 3, 3.5, 4, 5, 6, 7, 8, 9, 10, 11, 12, 13, 14, 15, 25]. For example, the average of all the NO_x/NO_y ratios in June, July and August of 1979-2012 with surface area densities between 0.1-0.4 $\mu m^2\ cm^{-3}$ is taken and plotted as one point with the x value equal to the average of the surface area densities of those points within the specified bin.

The values in red are these averages. The bins that had points with more than 50% of the surface area densities coming from before the 1990 with particularly low chlorine levels are highlighted in grey. The only points that this filtering affects are those with high surface area densities observed during the El Chichón period. One can see from this highlighting that these years don't follow the same trends as the other years- predominantly because the chlorine levels in the atmosphere are so much lower. These points can be ignored for the purpose of understanding the current changes in chemistry with higher chlorine levels more like those during the Mt. Pinatubo years. The red dashed line connects the relevant points in the figure. From looking at Figure 10, it is apparent that the variation in surface area density is a lot lower at 21mbar than it is at 100mbar because larger aerosols just don't make it up that far into the atmosphere and persist, thus the range of surface area density is different between the 21mbar and 100mbar plots.

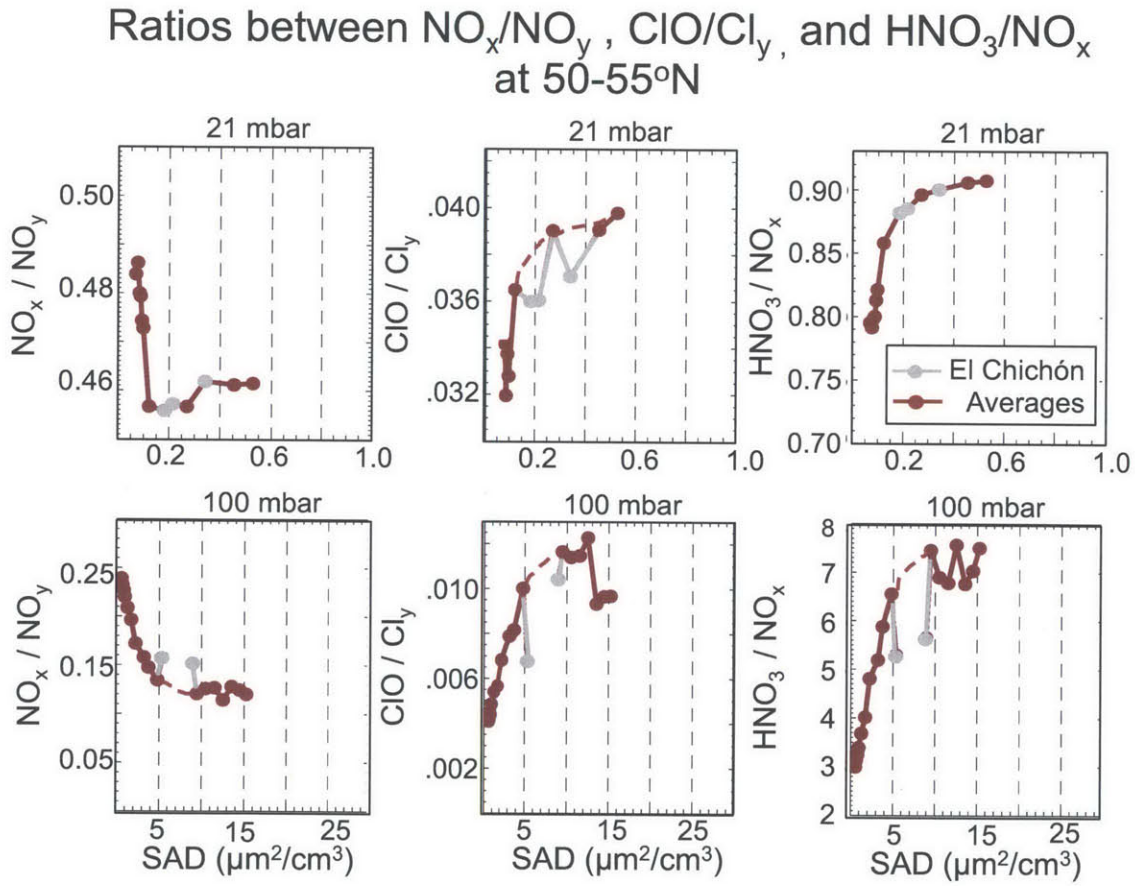

Figure 11: The ratios between NO_x/NO_y , ClO/Cl_y , and HNO_3/NO_x as a function of surface area density taken in June, July and August 1979-2012 when solar zenith angle is less than 45^o.

The first ratio shown is the NO_x/NO_y ratio which gives information on how much reactive nitrogen is available in the atmosphere. Figure 11 shows that the lowering of this ratio is very nonlinear and occurs rapidly as surface area density increases from 0-5 $\mu m^2\ cm^{-3}$ at 100mbar. The second ratio shown is the ClO/Cl_y ratio which gives information about how much more ClO is around to depleted ozone rather than in its reservoir species, $ClONO_2$ from the lowering of NO_x levels and the subsequent decrease in rate of reaction 10. This ratio also increases very nonlinearly for surface areas between 0-5$\mu m^2\ cm^{-3}$ at 100mbar. The third ratio shown is the HNO_3/NO_x ratio which gives information on how much HNO_3 there is in relation to reactive nitrogen. This ratio goes up with surface area density as the rate of the hydrolysis of N_2O_5 (22) goes up and decreases NO_x levels by pushing nitrogen from the less inert reservoir, N_2O_5 to the more inert reservoir, HNO_3. This ratio also changes very nonlinearly with surface area densities between 0-5 $\mu m^2\ cm^{-3}$ at 100mbar. We can see that at 21mbar, the nonlinearity of all of the ratios persists as well. However, the range of surface area densities over which the ratios drops is much lower with the major change happening between 0-0.2 $\mu m^2\ cm^{-3}$. Additionally, it must be noted that the absolute value of the change of the ratios at 21mbar is smaller than that of the ratios at 100mbar.

Table 1 shows how the average surface area density changed in the upper and lower stratosphere between the two SD-WACCM runs along with how much they would need to change in the lower stratosphere to match the Laramie, Wyoming measurements.

Run	21mbar	100mbar
SD-WACCM Clean	0.140	0.630
SD-WACCM Aerosols	0.191	1.087
Wyoming Adjusted	–	1.338

Table 1: Shown above are the average surface area densities ($\mu m^2\ cm^{-3}$) in June, July and August of 2009-2012 with a solar zenith angle less than 45^o. This data shows how the amount of aerosols increase between the two SD-WACCM runs, as well as how much those at 100mbar would change to be aligned with the average SAD measurements taken in Laramie, Wyoming.

Using the average surface area values in Table 1, the effect on the ratios given in Figure 11 can be predicted. Figure 12 marks the change in the ratios based on the change in average surface area density of the recent volcanic period 2009-2012 between the two SD-WACCM runs and the Wyoming measurements. The change in ratio is highlighted in blue for the difference in surface area density between the SD-WACMM runs with and without aerosols. The change between the SD-WACCM aerosol run and the Wyoming measurements is shown in yellow for the 100mbar level. The change in average aerosol surface area density is greatest between the two SD-WACCM runs, but the change in average surface area density needed to match the Wyoming measurements take place on a steeper part of the ratios curve. Thus, even though this change is smaller, it has a more pronounced effect on the lowering of NO_x levels and the increased activation of ClO than a

similar change would cause with lower SADs. At the 118mbar level, where the CCMI aerosol data set underestimates the Wyoming measurements by a factor of 2 or more, this effect is even more pronounced.

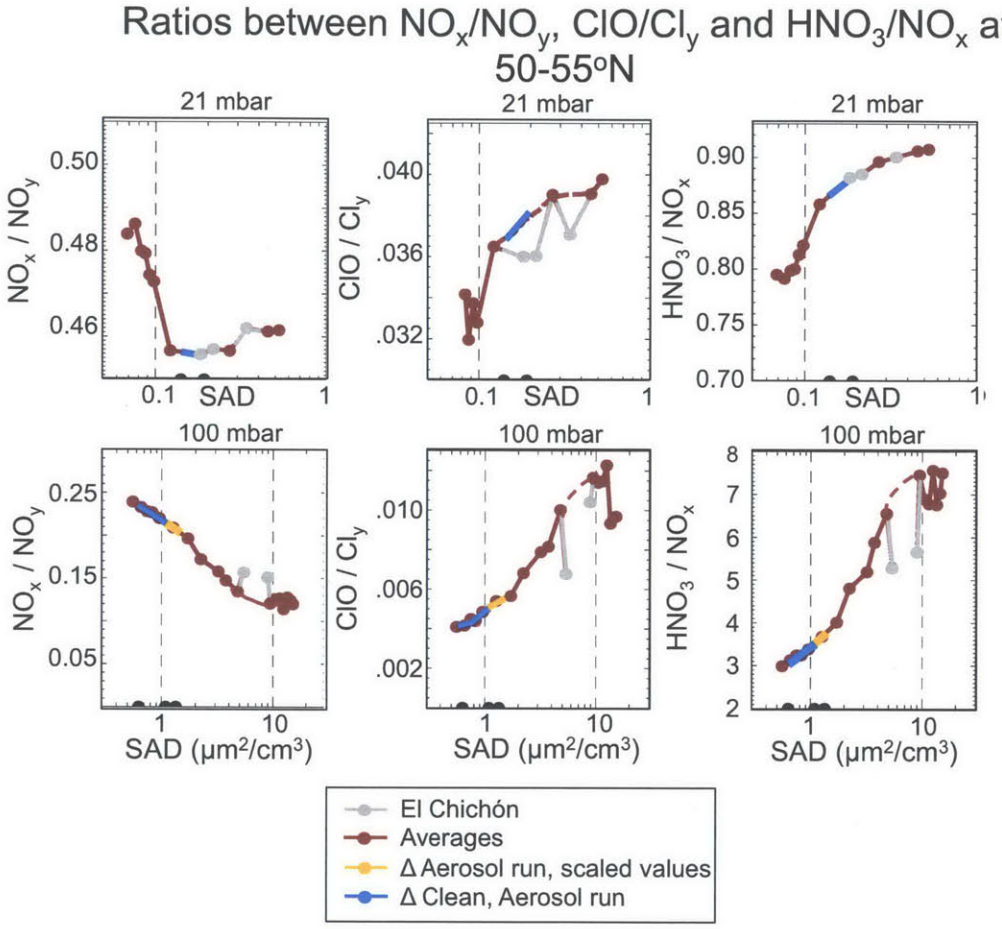

Figure 12: The ratios between NO_x/NO_y, ClO/Cl_y, and HNO_3/NO_x as a function of surface area density taken in June, July and August 1979-2012 when solar zenith angle is less than 45^o on a log scale. The difference in the average surface area density in the period 2009-2012 between the SD-WACCM run with aerosols and without is shown in blue. The difference in the average surface area density between the run with aerosols and that predicted from Laramie, Wyoming insitu measurements in yellow. Table 1 shows the changes in average surface area density.

Figure 12 shows the difference that even a small change in surface area density can have on the amount of NO_x and ClO. Using the scaling factor developed to describe the differences between the CCMI aerosols and Wyoming aerosol measurements, a prediction of ozone loss amounts at different levels in the stratosphere were made and those results shown in Figure 13. In order to make this estimate, a particular ozone anomaly was found in the historical period, 1979-2010, with

surface area and chlorine levels closest to those amounts. This anomaly was assumed to persist and was used to calculate the change from the clean run after 2005. The estimated ozone losses using the scaled aerosol data set are shown in green on the center panel of Figure 13alongside the two SD-WACCM runs. Scaled aerosols were used in the entire period from 2005-2012 after SAGE II measurements stopped informing the CCMI aerosol input. Figure 12 indicates that more ozone loss may have occurred in the lower stratosphere than initially predicted from the model because of the underestimations of surface area density by the CCMI aerosol data set.

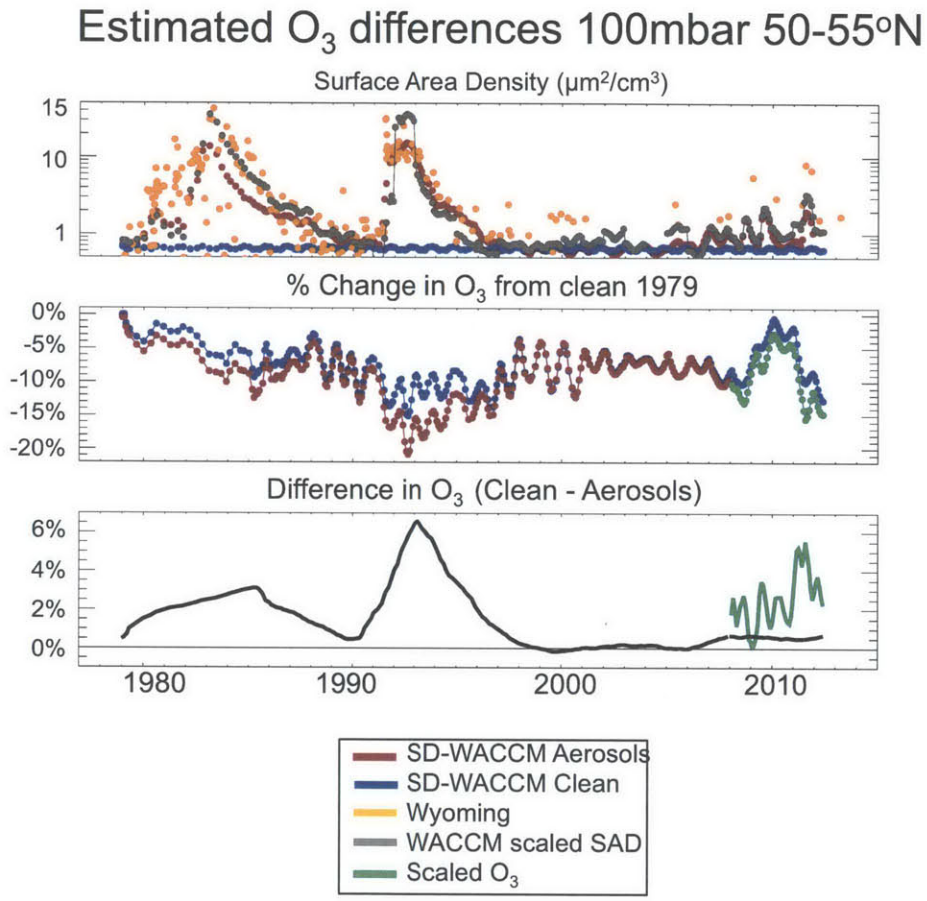

Figure 13: Ozone measurements and anomalies shown between the two SD-WACCM runs at 100mbar and the estimated ozone losses resulting from adjustments made to the scaling factor for surface area density.

Results like those in Figure 13 throughout 70mbar-120mbar in which the CCMI aerosols data set underestimates the Wyoming measurements, can give the corrected percent change in the column ozone values. The resulting percent change between the clean run of SD-WACMM and the predicted O_3 change using the scaled aerosols are shown in Figure 14. When compared to the original comparison of column ozone between the two SD-WACCM runs in ?? and seen in the

left panel, it can be seen that the scaled aerosols did affect the percent of ozone lost in the lower stratosphere. This figure indicates that the underestimation of volcanic surface area densities did have a significant effect on ozone values throughout the column. The estimated effect on ozone loss in the lower stratosphere after the Nabro eruption in 2011 is seen to rival that of the losses seen in the years following the El Chichón eruption around 1984. However, the entire period 2009-2012 with adjusted aerosols sees of 2-2.5% more ozone loss in the lower stratosphere than from the clean run. The initial run using the CCMI aerosols only showed ozone losses of around 0.5% at those levels again underscoring the effects that small surface area density changes can have on total ozone.

Particularly, since the CCMI aerosol data set only underestimates surface area densities in the lower stratosphere but not the upper stratosphere, the model then only underestimates the amount of ozone lost in the lower stratosphere, but doesnt significantly underestimate the amount of ozone produced in the upper stratosphere. This means that after integrating through the column, we would expect more ozone lost after correcting the aerosol surface area densities in the later period than was shown initially in Figure 8. Ultimately, the adjusted ozone values shown in **??** indicate that the recent small, volcanic eruptions may have lowered ozone column levels more than expected. These losses may have had enough of an effect to cover the increases in ozone from declining chlorine levels, and may be part of the reason column ozone recovery has been stagnant while being expected to recover.

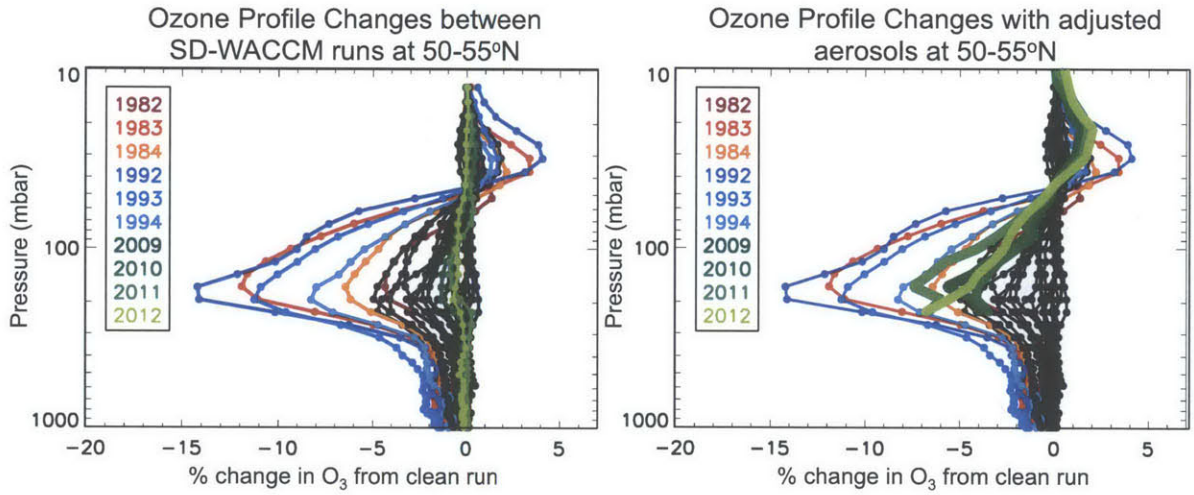

Figure 14: Ozone anomalies shown between the SD-WACCM run without aerosols and the scaled CCMI aerosols throughout the O3 column.

5 Conclusions

It has been shown, that the CCMI aerosol data set tends to underestimate the true surface area density in the lower stratosphere between the local tropopause and approximately 70mbar. Such error is unaccounted for after 2005 and may result from errors in back calculating surface area densities from different aerosol extinction measurements after the CCMI aerosol data set stops using SAGE II retrievals and begins using CALIPSO retrievals. This result is important for future users intending to use the CCMI aerosol data set as input into chemistry climate models- especially for those involving heterogenous reactions in the lower stratosphere. Using this data set as input to SD-WACCM along with a separate run done using only background aerosol values, it was initially shown that the recent volcanoes in the period 2008-2012 had little effect on total column ozone or local ozone loss and production in the lower and upper stratosphere, respectively.

However, the catalytic cycles leading to ozone loss and production are shown to respond nonlinearly to changes in surface area density with most of the change happening in the range from 1-3$\mu m\ cm^{-3}$. Thus, even small errors in measuring surface area density in the lower stratosphere, can have large effects on the amount of ozone loss seen in the area. Because the volcanic eruptions between 2008-2012 were only ejecting small particles into the atmosphere in the center of the very sensitive area for ozone loss chemistry, even small errors in the satellite measurement could cause very different effects on ozone. Aerosol surface area densities are particularly hard to measure with satellites in the lower stratosphere. Therefore, our results underline the importance of continuous ground-based measurements of surface area densities for verification of satellite retrievals.

After accounting for the underestimation in the CCMI aerosol data set by using a scaling factor derived from measurements of surface area density in Laramie, Wyoming, the ozone loss through the column was recalculated and found to be significant in the recent volcanic period from 2008-2011. The results indicate that the initial model run which showed only a slight effect on the ozone column from the recent volcanoes underestimated the total ozone loss from these volcanoes because the aerosols themselves were underestimated. After the large Nabro eruption in 2011, lower stratospheric ozone was shown to decrease by nearly 4-5% more than it would have if there were no aerosols during this time. These decreases are on the same order of magnitude as those seen in the years following the El Chichón eruption where lower chlorine levels diminished its effect on stratospheric ozone although it ejected more aerosols. Ultimately, we have shown that even small perturbations to atmospheric aerosols can cause large changes in the chemistry of the stratosphere. This is an important result for consideration in global warming solutions involving injections of sulfuric acid particles into the stratosphere to reflect incoming radiation and lower surface temperature. In such a scenario, continuous, small injections of these particles would have to occur to maintain the surface temperature and would likely be released all at once- very similar to a scenario with small, continuous volcanic eruptions. Our results indicate that even such small injections of particles have the capacity to dramatically lower ozone levels in the lower stratosphere.

Thus, such a geoengineering solution could have major impacts on the ozone layer.

Finally, these results estimating ozone column losses from the adjusted CCMI aerosol data set were found through crude estimations using a well-established framework of ozone relevant nonlinear chemistry. Future work includes rerunning SD-WACCM using a scaled CCMI aerosol data set with the values herein derived to see the true effect on ozone without having to estimate the changes we would see by using this data set. By storing relevant rate constants when running SD-WACCM we could also complete a more thorough analysis of which reactions specifically are effected the most, and by what order of magnitude. Although this project was an important first step in understanding that the potential effect that small volcanoes can have on stratospheric ozone is large, a more thorough analysis would allow for more concrete results.

6 References

Arfeuille, F. F., Luo, B. P., Heckendorn, P. P., Weisenstein, D. D., Sheng, J. X., Rozanov, E. E., & ... Peter, T. T. (2013). Modeling the stratospheric warming following the Mt. Pinatubo eruption: uncertainties in aerosol extinctions. Atmospheric Chemistry & Physics, 13(22), 11221-11234. doi:10.5194/acp-13-11221-2013

Austin, J., et al. (2010), Decline and recovery of total column ozone using a multimodel time series analysis, J. Geophys. Res., 115, D00M10, doi:10.1029/2010JD013857.

Bourassa, A. E., et al., 2012: Large volcanic aerosol load in the stratosphere linked to Asian monsoon transport. Science, 337, 78-81.

Brasseur, G. Granier, C., & Walters, S. (n.d). Future changes in stratospheric ozone and the role of heterogeneous chemistry. Nature, 348(6302), 626-628.

Brasseur, G., & Solomon, S. (2005). Aeronomy of the middle atmosphere : chemistry and physics of the stratosphere and mesosphere Guy P. Brasseur and Susan Solomon. Dordrecht : Springer, 2005.

Deshler, T., Hervig, M., Hofmann, D., Rosen, J., & Liley, J. (2002). Thirty years of in situ stratospheric aerosol size distribution measurements from Laramie, Wyoming (41 degrees N), using balloon-borne instruments. Journal Of Geophysical Research-Atmospheres, 108(D5).

Eyring, V., et al., 2006. Assessment of temperature, trace species, and ozone in chemistryclimate model simulations of the recent past, J. Geo phys. Res., 111, D22308, doi:10.1029/2006JD007327.

Eyring, V., Cionni, I., Bodeker, G., Charlton-Perez, A., Kinnison, D., Scinocca, J.,& ... Yamashita, Y. (2010a). Multi-model assessment of stratospheric ozone return dates and ozone recovery in CCMVal-2 models. Atmospheric Chemistry And Physics, 10(19), 9451-9472.

Eyring, V., et al., 2010b. Sensitivity of 21st century stratospheric ozone to greenhouse gas scenarios. Geophysical Research Letters, 37, L16807.

Fahey, D., Sawa, S. Woodbridge, E., Tin, P., Wilson, J., Jonsson, H., & Chan, K. (n.d). In-situ measurements constraining the role of sulfate aerosols in mid-latitude ozone depletion. Nature, 363(6429), 509-514.

Jacob, D. J. (1999). Introduction to atmospheric chemistry Daniel J. Jacob. Princeton, N.J. : Princeton University Press, c1999.

Montzka, S. A., E. J. Dlugokencky, and J. H. Butler, 2011: Non-CO(2) greenhouse gases and climate change. Nature, 476, 43-50.

Nagai, T., B. Liley, T. Sakai, T. Shibata, and O. Uchino, 2010: Post-Pinatubo Evolution and Subsequent Trend of the Stratospheric Aerosol Layer Observed by Mid-Latitude Lidars in Both Hemispheres. Sola, 6, 69-72.

Neely, R. R., et al., 2013: Recent anthropogenic increases in SO2 from Asia have minimal impact on stratospheric aerosol. Geophysical Research Letters, doi:10.1002/grl.50263.

Robock, A. (2000), Volcanic eruptions and climate, Reviews of Geophysics, 38 (2), 191219.

Molina, M. J., & Rowland, F. S. (1974). Stratospheric sink for chlorofluoromethanes: chlorine atomc-atalysed destruction of ozone. Nature, 249(5460), 810. doi:10.1038/249810a0

Seinfeld, J. H., & Pandis, S. N. (2006). Atmospheric chemistry and physics : from air pollution to climate change John H. Seinfeld, Spyros N. Pandis. Hoboken, N.J. : Wiley, 2006.

Solomon, S. S., Portmann, R. W., Garcia, R. R., Thomason, L. W., Poole, L. R., & McCormick, M. P. (1996). The role of aerosol variations in anthropogenic ozone depletion at northern mid-latitudes. Journal Of Geophysical Research, 101(D3), 6713-6727.

Thomason, L. W., Poole, L. R., & Deshler, T. T. (1997). A global climatology of stratospheric aerosol surface area density deduced from Stratospheric Aerosol and Gas Experiment II measurements: 1984-1994. Journal Of Geophysical Research, 102(D7), 8967-8976.

Vernier, J. P., et al., 2011: Major influence of tropical volcanic eruptions on the stratospheric aerosol layer during the last decade. Geophysical Research Letters, 38, L12807.

Wennberg, P. O., Cohen, R. C., Stimpfle, R. M., Koplow, J. P., Anderson, J. G., Salawitch, R. J., & ... Wofsy, S. C. (1994). Removal of Stratospheric O3 by Radicals: In Situ Measurements of OH, HO2, NO, NO2, ClO, and BrO. Science, (5184), 398. doi:10.2307/2885319

7 Appendices

7.1 Appendix A

Level (mbar)	2005	2006	2007	2008	2009	2010	2011	2012
10.284921	0.718659							
12.46015	0.767302							
15.05025	0.945216					0.530832		
18.124349	0.883108	0.215085	0.822776	0.335633	1.37434	0.729223		
21.761005	0.763989	0.409084	0.83597	0.364473	1.04681	0.603634	0.557809	0.490878
26.04911	0.764657	0.619468	0.943369	0.576082	0.89327	0.409988	0.520505	0.68117
31.088909	0.830652	0.679805	1.02864	0.806117	1.29864	0.454828	0.587809	0.704247
36.99271	0.9421	0.565968	0.954514	0.838569	1.3496	0.471938	0.710855	0.713269
43.909661	0.868208	0.584723	0.837186	0.800803	1.18621	0.490843	0.668514	0.797279
52.01591	0.909131	0.654929	0.714133	0.871798	1.03418	0.565623	0.546545	0.847601
61.495658	1.04505	0.71281	0.749934	1.02291	0.914671	0.67992	0.494814	0.915041
72.557859	0.960356	0.836857	0.913231	1.0932	1.03261	0.836535	0.605834	0.966702
85.439015	1.07425	0.874361	1.13644	1.12778	1.02117	1.0979	1.09173	1.28984
100.51436	1.5947	0.827985	1.18293	1.03848	1.09063	1.31914	1.66908	1.74697
118.25	1.84622	0.927101	1.3155	1.07336	1.11979	1.7299	2.04757	2.41014
139.115	1.6611	0.964368	1.63361	1.01989	1.1166	1.98104	6.00864	2.15812
163.6615	1.5518	0.859671	1.83117	0.922181	1.06205	2.57642	7.46624	1.56457
192.54102	1.31522	0.713497	1.6037	0.924493	1.0047	2.89942	4.00521	1.39558
226.51354	1.23977	0.736219	1.94383	0.840181	1.00717	2.74568	3.6201	1.17497
266.47905	1.26062	0.865317	4.14963	1.31183		2.8597	3.3273	1.39762
312.79158		0.899945	5.08234	2.13597		15.8132	3.8366	2.24033
356.2501		1.10648	3.24079	2.19054		14.5591	3.985	4.70935
393.7501							2.948	

Figure 15: The scarling factor in $\mu m^2 cm^{-3}$ by which the CCMI surface area densities must be multiplied in order to match the Wyoming measurements in June, July and August as a function of pressure.

Year	21mbar	31mbar	43mbar	52mbar	61mbar	72mbar	85mbar	100mbar	118mbar
2005	2.280149091	1.613582273	0.261055382	-0.442822218	-1.172701636	-1.695697818	-2.111126364	-2.388519091	-2.986780909
2006	0.687842658	0.850890483	0.186698417	-0.210407069	-0.298175258	-0.235662892	-0.421294733	-0.788479917	-0.974174
2007	1.880385833	1.537232333	0.113200467	-0.375739567	-1.121093	-1.715086667	-1.88478425	-2.311978333	-3.535948333
2008	1.06211325	1.066874108	0.029651408	-0.333445227	-0.912393417	-1.233793833	-1.330609925	-2.137294167	-2.870141417
2009	1.375894667	1.089133167	-0.015896892	-0.202812675	-0.725218417	-1.04671325	-1.460728417	-2.295379167	-3.463864333
2010	1.860136667	1.3412285	0.039522525	-0.448566333	-1.119407833	-1.633370833	-1.018366617	-2.017315833	-2.9599425
2011	1.778569	1.515519333	0.090322417	-0.499023833	-1.328338167	-2.144135833	-3.048625	-4.0986925	-5.748885
2012	2.014998333	1.633216667	0.034666277	-0.614466	-1.334303333	-1.940725	-2.375805	-2.675838333	-3.284038333

Figure 16: In this table is the percentage by which the ozone column using adjusted aerosols is different from the clean run of SD-WACCM. These are the values plotted as a function of pressure in the right most panel of Figure 14. Negative values indicate that ozone decreased at that level and the opposite for positive values.